Design and Control of an Ultrasonic Motor Capable of Generating Multi-DOF Motion

Kenjiro Takemura and Takashi Maeno

***Abstract*—A multi-degree-of-freedom (DOF) ultrasonic motor consisting of a bar-shaped stator and a spherical rotor was developed. It can generate 3-DOF rotation of the rotor around perpendicular axes using bending vibrations and a longitudinal vibration of the stator, which was designed using finite element analysis. From the simulated driving characteristics, a control method for the ultrasonic motor was proposed. Following this, the driving characteristics of the motor under open-loop control and closed-loop control were measured experimentally. Multi-DOF position control of the rotor was achieved successfully using the proposed control method.**

***Index Terms*—Finite element analysis, multi-DOF, ultrasonic motor, vibration.**

I. Introduction

GENERALLY, electromagnetic motors have been used in order to construct a multi-degree-of-freedom (DOF) motion unit. However, in such units, the number of the motors must be equal to or larger than the number of DOFs of the motion unit, because general electromagnetic motors generate only single-DOF rotation. What is worse, reduction devices must be connected to electromagnetic motors in order to obtain large torque, which increases the total volume and weight of the multi-DOF motion unit.

As a result, the need for multi-DOF actuators is increasing. If multi-DOF actuators are used, the total volume and weight of the motion unit become smaller. Hence, a number of different actuators capable of generating multi-DOF motion have been developed or proposed in recent years [1]. Roth *et al.* proposed a 3-DOF variable reluctance spherical wrist motor [2], which can generate 3-DOF motion using reluctance forces between coils located in the stator and magnets in the rotor. Yano developed a spherical stepping motor [3] consisting of a rotor with three stators arranged around it. 3-DOF motion of the rotor can be generated.

The examples mentioned above use the principle of the electromagnetic motor, and therefore, motor geometry is complicated and the range of movement of the rotor is insufficient. On the other hand, an ultrasonic motor has excellent characteristics such as high torque at low speed, high stationary limiting torque, absence of electromagnetic radiation, and simplicity of design. Therefore, a multi-DOF actuator using the principle of an ultrasonic motor is proposed.

Manuscript received July 7, 2000; revised April 3, 2001. Recommended by Technical Editor C. H. Menq. This work was supported in part by Canon Inc.

K. Takemura is with the Graduate School of Science and Technology, Keio University, Yokohama, 223-8522 Japan (e-mail: kenjiro@mmm-keio.net).

T. Maeno is with the Department of Mechanical Engineering, Keio University, Yokohama, 223-8522 Japan (e-mail: maeno@mech.keio.ac.jp).

Publisher Item Identifier S 1083-4435(01)10735-0.

Bansevicius developed a piezoelectric multi-DOF actuator [4] with a cylindrical stator (vibrator) and a spherical rotor. The rotor rotates around three perpendicular axes by combining certain natural vibration modes of the stator. Amano *et al.* developed a multi-DOF ultrasonic actuator [5] in which a spherical rotor rotates around three perpendicular axes using the three natural vibration modes of a stator. Toyama constructed a spherical ultrasonic motor [6] consisting of three ring-shaped stators (vibrators) and a spherical rotor. 3-DOF rotation of the rotor can be generated combining the driving forces from each stator. Sasae *et al.* developed a spherical actuator [7] where a 3-DOF motion unit is constructed using truss arranged PZTs. The 3-DOF rotation of a spherical rotor is generated using the three-DOF motion unit arranged around the rotor.

Although the actuators [4]–[7] can generate multi-DOF motion of rotor as described above, they cannot replace a combination of general electromagnetic motors because of their small output torque, low controllability and nonsimplicity of design. In order to solve these issues, the geometry of a multi-DOF ultrasonic motor must be designed precisely and new control method must be proposed.

The authors have developed a new type of ultrasonic motor capable of generating multi-DOF motion. The multi-DOF ultrasonic motor generates multi-DOF rotation of a spherical rotor using the three natural vibration modes of a bar-shaped stator. In this paper, the principle and geometry of the multi-DOF ultrasonic motor are described in Section II. Then, a control method for the multi-DOF ultrasonic motor is proposed in Section III. The construction of the multi-DOF ultrasonic motor and the measuring devices are described in Section IV. The experimental results of the open-loop control tests and the closed-loop control tests are given in Section V. Then in Sections VI and VII, the discussion and conclusion of this study are given, respectively.

II. Design of Vibration Modes and Geometry

A. Vibration Modes

An ultrasonic motor is a frictionally driven motor. It generally consists of a stator (vibrator) and a rotor [8]–[10]. The energy of the natural vibrations of the stator is transmitted to the rotation of the rotor by the frictional force between the rotor and stator. Most ultrasonic motors utilize two natural vibration modes of the stator in order to generate single-DOF rotation of the rotor. The oval trajectories of points on the stator rotate around a specific axis by combining the two natural vibration modes. Then, the rotor, which is in contact with the stator, rotates around the specific axis. We extend this idea to multi-DOF motion, such that multi-DOF motion can be generated by making the axis

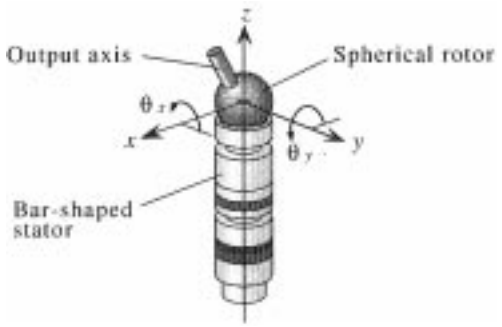

Fig. 1. Schematic view of multi-DOF ultrasonic motor.

of the oval trajectories vary voluntarily. Three natural vibration modes with directions of vibration perpendicular to each other should be used in order to produce voluntary oval trajectories of contact points and to make the rotor rotate around any axis. Namely, a stator that meets following requirements must be designed:

1) natural frequencies of three vibration modes correspond;
2) vibrating directions of the vibration modes are perpendicular each other;
3) geometry of the stator must be simple for easy production;
4) three vibration modes must be lower natural vibrations for not exciting other needless modes.

Geometry of the stators and vibration modes meeting the above requirements are not the only one, however, we adopt a bar-shaped stator and its bending and longitudinal vibrations, because the geometry of the stator and the vibration modes are simple.

The multi-DOF ultrasonic motor we propose consists of a bar-shaped stator and a spherical rotor as shown in Fig. 1 (the diameters of the stator and rotor are both 10 mm, and the length of the stator is 31.85 mm). The three axes (x, y, z) are defined in this paper as shown in Fig. 1. Fig. 2 shows the driving principle of the multi-DOF ultrasonic motor. The rotor can rotate around three perpendicular axes. A longitudinal vibration and two bending vibrations of the stator are used as shown in Fig. 2. Fig. 2(a) shows the natural vibration modes of the stator that are used when the rotor rotates around the z axis. Figs. 1 and 3 show the second bending mode of the stator in the zx plane (mode A), and Figs. 2 and 4 show the second bending mode of the stator in the yz plane (mode B). When these two natural vibration modes, A and B, are combined at a phase difference of 90°, the tip of the stator rotates around the z axis. Then, the spherical rotor in contact with the stator's head also rotates around the z axis by frictional force. Fig. 2(b) shows the natural vibration modes used when the rotor rotates around the x axis. Figs. 1 and 3 show the first longitudinal mode of the stator along the z axis (mode C), and Figs. 2 and 4 show the mode B. When these two natural vibration modes, B and C, are combined at a phase difference of 90°, the tip of the stator rotates around the x axis. Then, the spherical rotor also rotates around the x axis due to frictional force. The rotor rotates around the y axis when the mode A and the mode C are combined in the same way as the case of Fig. 2(b). The point to notice is that the natural frequencies of these three natural vibration modes, A, B, and C, should correspond.

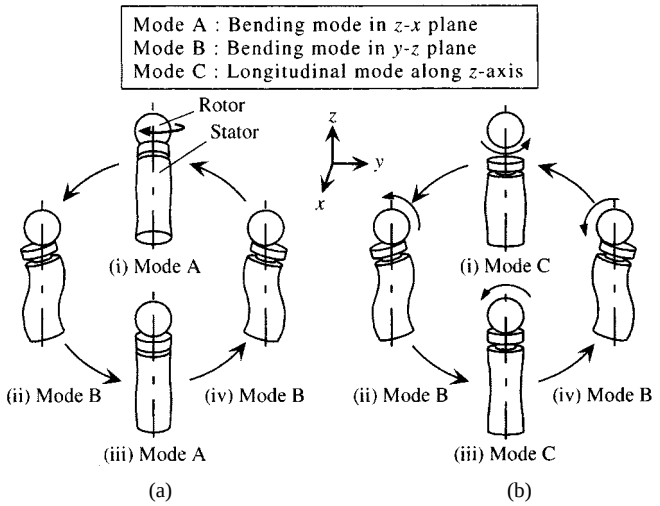

Fig. 2. Driving principle of a multi-DOF ultrasonic motor. (a) Around the z axis. (b) Around the x axis.

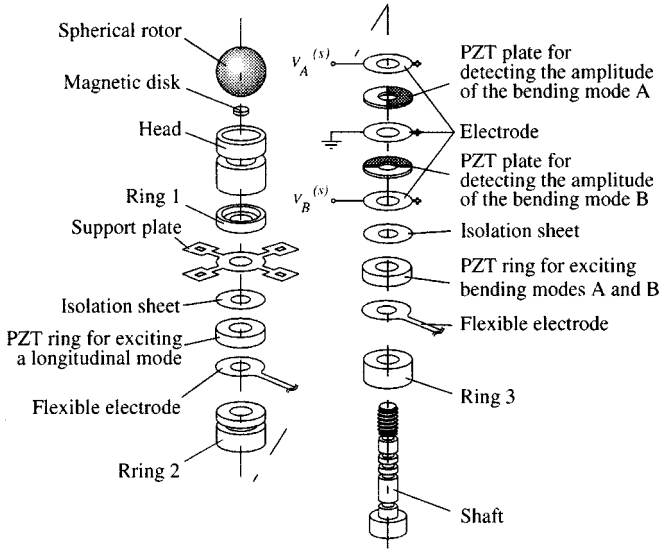

Fig. 3. Geometry of the multi-DOF ultrasonic motor.

B. Geometry

The natural frequencies of the bending mode and the longitudinal mode of the stator must correspond, as mentioned in Section II-A. Accordingly, geometry of the real stator is designed using the finite element analysis in order to calculate the shapes and frequencies of the natural vibration modes, considering the following requirements:

1) the bar-shaped stator should be, so to say, the Langevin vibrator for easy construction;
2) piezoelectric ceramics (PZT) for exciting the vibration modes should be located at where the normal strains are high when the vibration modes are excited;
3) mechanism for enlarging vibration amplitude such as constriction should be located in the stator;
4) support mechanism that has little influence on the vibration modes should be provided.

Fig. 3 shows the geometry of the designed multi-DOF ultrasonic motor. The rotor is made of stainless steel. The stator consists primarily of head, rings, stacked PZT rings, and a shaft.

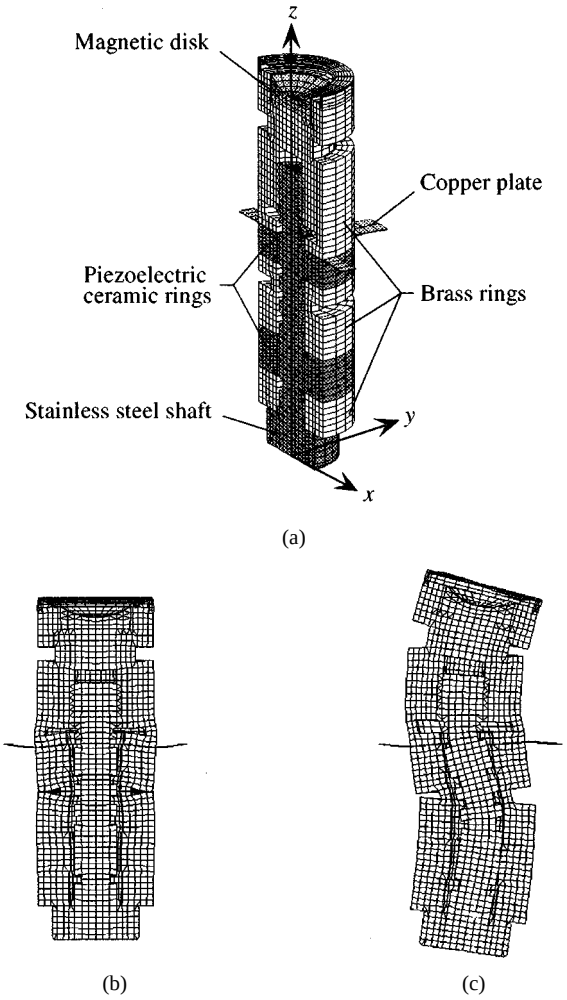

Fig. 4. Finite element model and calculated natural modes of the stator. (a) Finite element model of the stator. (b) First longitudinal mode. (c) Second bending mode.

The stator head, rings, and shaft are made of nickel-plated brass, brass, and stainless steel, respectively. Geometry of constrictions of the stator head and the rings are designed to make the natural frequencies of the vibration modes correspond and to amplify the vibration amplitude. Namely, the natural frequencies of the bending mode and the longitudinal mode can be modified by changing the diameters of the constrictions at the stator head and the ring. We adopt the diameter and length of constrictions as parameters for frequency adjustment, so that the optimum dimension of the stator, which made three natural frequencies correspond, was determined by repeating FE analysis. The stacked PZT rings are provided to excite the natural vibrations of the stator. The polarization direction of the PZT ring for longitudinal mode is uniform. The PZT for bending mode is divided into quarter parts by diameters. The polarization directions of the opposite areas are opposite each other. Flexible electrodes shown in Fig. 3 are located to apply the voltage to the PZT rings. The shaft is screwed to the stator head in order to construct the stator as the Langevin vibrator. The ends of the cross-shaped support plate are fixed on a pedestal in order to brace the stator, and a magnetic disk is placed at the top of the stator head. A normal load between the rotor and stator is applied by the magnetic disk. The amplitudes of the vibrations can be detected using the PZT plates shown in Fig. 3. The polarization directions of the two components (colored gray and white) oppose each other.

Fig. 4 shows the geometry and natural modes of the stator designed considering the design requirements mentioned above. Fig. 4(a) shows the finite element model of the stator, which is a half-columnar model because the bending mode and the longitudinal mode of the bar-shaped stator are geometrically symmetric with respect to the $z\,x$ plane. Fig. 4(b) and (c) show the calculated first longitudinal mode and the calculated second bending mode of the stator, respectively. The calculated natural frequencies of these modes are equal, about 43 kHz. If the amplitudes of the natural vibrations are 1 μm, the estimated rotational speeds of the rotor around the x (y) and z axes are 405 and 577 r/min, respectively, calculated from the velocity of the contact point between the rotor and stator. Then, the estimated torque around the x (y) and z axes are 15 and 12 mNm, respectively, when the coefficient of friction and the normal load between the rotor and stator are assumed to be 0.5 and 6 N, respectively, as calculated using the following equation:

$$T = \mu F r \tag{1}$$

where T is the torque, μ is the coefficient of friction, F is the normal load between the rotor and stator, and r is the moment arm length.

III. Design of Control System

A. Assignment of the Operating Parameter

Three AC signals are input to each PZT ring in order to excite the second bending vibration mode and the first longitudinal vibration mode of the stator. The frequencies, the voltages and the phase differences of input signals are all potential operating parameters for controlling the motion of the multi-DOF ultrasonic motor. For practical single-DOF ultrasonic motors [8], [9], the frequencies of input signals are varied as operating parameters. However, in case of the multi-DOF ultrasonic motor, the frequencies are unsuitable operating parameters as described later. Therefore, we must determine the operating parameter of the multi-DOF ultrasonic motor considering the following requirements:

1) rotational speeds around the three perpendicular axes must be able to be varied independently;
2) vibration characteristics of the stator, such as natural frequencies and quality factors, must not change even when the value of the operating parameter is varied;
3) the rotational direction must be able to be changed.

Due to requirement 1), we can find that the frequencies of the input signals are not suitable operating parameters for the multi-DOF ultrasonic motor because the rotational speed around the three perpendicular axes cannot be varied independently when the frequencies are varied. With respect to requirement 2), we can also see that the voltages of the input signals cannot be varied as operating parameters because the vibration characteristics of the natural vibration modes change independently, as known from experience. In other words, the natural frequencies of the modes, which have different modal masses and modal stiffness, do not shift equally. So, the phase difference of the input signals seems to be a suitable operating parameter. In order

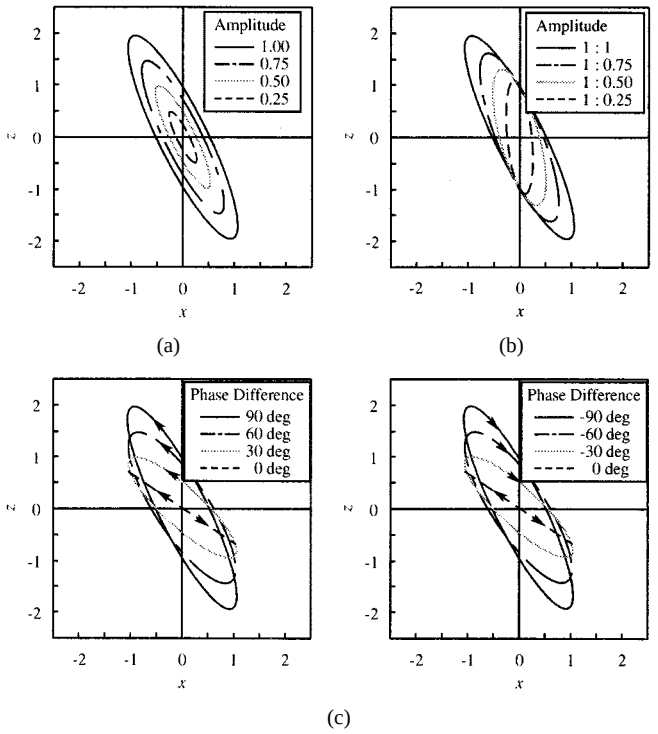

Fig. 5. Simulated oval trajectories at the contact interface of the bar-shaped stator. (a) Frequencies are varied. (b) Voltage is varied. (c) Phase difference is varied.

to investigate the suitability of this option, the oval trajectory of the contact point between the rotor and stator is simulated using the modes' shapes, which are obtained by the finite element analysis.

Fig. 5 shows the simulated oval trajectory when (a) the frequencies of the input signals are varied; (b) the voltage of the input signal for the second bending mode is varied; and (c) the phase difference between the input signals is varied. The values of the vertical and horizontal axes in Fig. 5 represent the normalized displacements along the z and x axis, respectively. The size of the oval trajectory determines the rotational speed of the rotor. From Fig. 5, it is seen that the rotational speed of the rotor can be varied when the values of the each parameter are changed. Furthermore, the rotational direction is changed simply by changing the sign of the phase difference. In other words, only the phase difference of the input signals meets requirement 3). If the phase difference is varied as an operating parameter, the efficiency of the multi-DOF ultrasonic motor will decrease, but this is not an important consideration for this study.

From the above discussion, we conclude that the phase difference of the input signals is a suitable operating parameter for the multi-DOF ultrasonic motor.

B. Proposition of Control Method

A control method for the multi-DOF ultrasonic motor is proposed in this section. The rotor's rotation around one axis is considered in the following discussion, although the proposed methods can be used when the rotational axis is extended to three perpendicular axes.

First, a speed-control method for the multi-DOF ultrasonic motor is proposed. The rotational speed and rotational direction

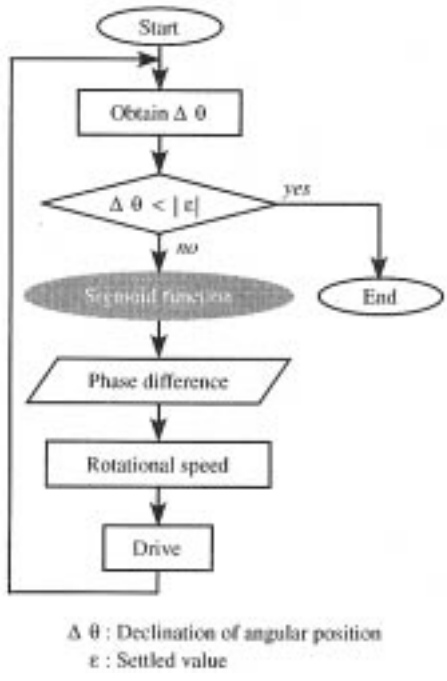

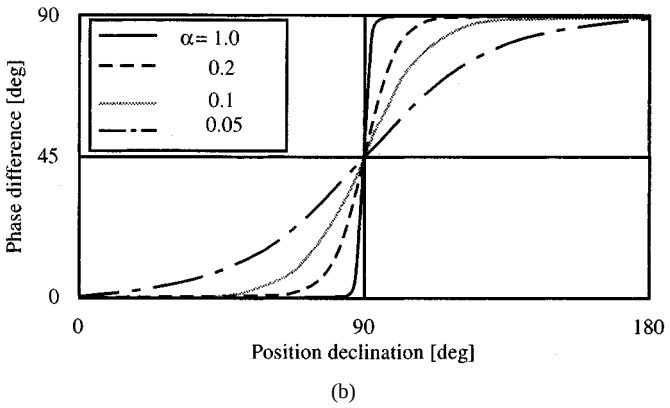

Fig. 6. Position control algorithm. (a) Flow chart. (b) Relationship between the position declination and the phase difference (sigmoid function).

of the rotor can be varied by changing the phase difference between the input signals, because the oval trajectory of the contact point on the stator is changed as shown in Fig. 5(c). So, the rotational speed including the rotational direction can be controlled using a proportional controller as shown in the following equation:

$$\Delta\phi = K_p \cdot \Delta N \tag{2}$$

where, $\Delta\phi$ is the phase difference, ΔN is the declination of rotational speed, and K_p is the proportional feedback gain. Then, if the absolute value of the declination of rotational speed is large, the absolute value of phase difference also becomes large by (2), however the absolute value of phase difference is within 90°.

Next, a position-control method for the multi-DOF ultrasonic motor is proposed. In order to make the response time short, the rotational speed must be varied according to the declination of the angular position of rotor. Namely, the rotational speed must be large when the declination of the angular position is large. A proposed position control algorithm is shown in Fig. 6(a). The

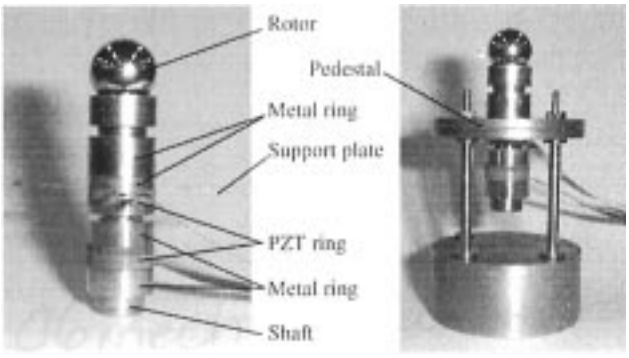

(a) (b)

Fig. 7. (a) Multi-DOF ultrasonic motor. (b) Multi-DOF untrasonic motor fixed on a pedestal.

following sigmoid function is used to make the phase difference vary according to the declination of rotor position:

$$|\Delta\phi| = 90 \cdot \frac{1}{1+\exp(-\alpha(\Delta\theta - M))} \tag{3}$$

where $\Delta\phi$ is the phase difference, $\Delta\theta$ is the declination of the angular position, and α and M are the parameters of the sigmoid function. The rotational speed becomes large when the declination of the angular position is large by using the sigmoid function for control. Furthermore, the relationship between the declination and the phase difference can be easily varied by changing the sigmoid function parameters α and M, as shown in Fig. 6(b).

IV. Construction

A. Construction of the Multi-DOF Ultrasonic Motor

Fig. 7(a) shows the multi-DOF ultrasonic motor that was built according to the geometry designed in Section II-B. Fig. 7(b) shows the multi-DOF ultrasonic motor fixed on a pedestal designed for the experiment. For practical application, the pedestal should be smaller. The diameter and the height of the stator are 10 and 31.85 mm, respectively, and the diameter of the rotor is 10 mm. The measured natural frequencies of the second bending mode and the first longitudinal mode are both around 40 kHz, which is about 7.5% lower than the calculated values. The difference between the calculated and the measured natural frequencies is due to the fact that the boundary between the parts of the stator and the flexible electrodes was not modeled. However, this does not matter because the measured natural frequencies of the bending mode and the longitudinal mode are almost the same.

B. Construction of the Measuring Device for Driving Characteristics

The driving principle of the multi-DOF ultrasonic motor around the z axis is the same as that of practical ultrasonic motors [8], [9]. On the other hand, the driving principles around the x and y axis are different from those of practical ultrasonic motors. The driving principle employed for the z axis is the traveling wave driving principle, and that for the x and y axis is the standing wave driving principle [10]. Therefore, it is necessary for the driving characteristics of the multi-DOF ultrasonic motor around the y (x) axis to be measured precisely in this paper. In order to measure the driving characteristics around the y (x) axis, the measuring device shown in Fig. 8(a) was built. The rotational axis of the rotor around the y (x) axis is provided by a shaft. A normal load between the rotor and stator is applied by coil springs arranged under a pedestal, and its value can be adjusted by turning the screw shown in Fig. 8(a). The rotational speed around the y (x) axis is measured using a rotary encoder connected to the shaft. The output torque around the y axis is applied using a weight attached to a string that is reeled using a pulley.

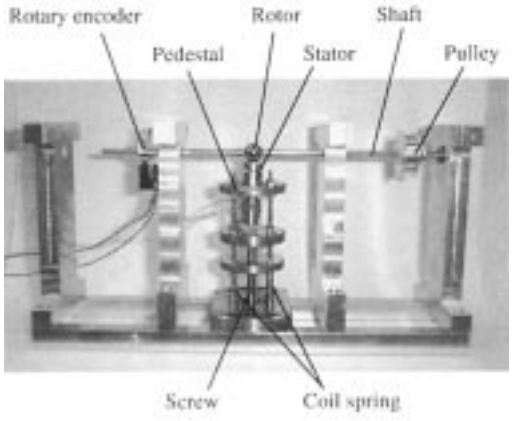

(a)

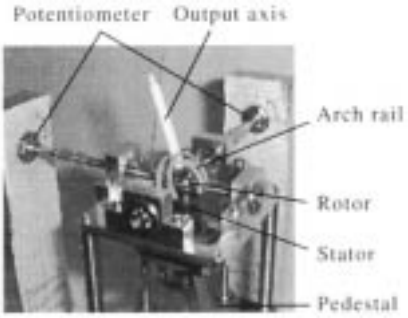

(a)

Fig. 8. (a) Measuring device for the driving characteristics around the *y* axis. (b) Multi-DOF position sending device

C. Construction of the Multi-DOF Position-Sensing Device

The multi-DOF ultrasonic motor can generate a multi-DOF rotation of the spherical rotor. Accordingly, the multi-DOF position of the rotor must be measured in order to control the motion of the rotor. For this, a multi-DOF position-sensing device was built. The angular positions of the rotor around the perpendicular axes were measured using the multi-DOF position-sensing device shown in Fig. 8(b). An output axis is connected to the rotor, and then it is inserted into the arch rails. The angular positions are measured using potentiometers, which are attached to each spindle of the arch rails.

V. Experimental Result

A. Results for Open-Loop Control Experiment

The experimental results for open-loop control are as follows. The basic experimental conditions are shown in Table I.

TABLE I
BASIC EXPERIMENTAL CONDITIONS

Frequency [kHz]	Same as natural frequencies of the modes
Voltage for bending mode [V]	20
Voltage for longitudinal mode [V]	10
Phase difference [deg]	90

1) Relationship Between Frequency and Rotational Speed: Fig. 9(a) shows the relationship between frequencies and rotational speed measured using the device shown in Fig. 8(a). It can be seen form Fig. 9(a) that the peak rotational speed is obtained when the frequencies of the input signals are about 40 kHz, that is, the natural frequencies of the first longitudinal mode and the second bending mode. The relationship between the frequencies and the rotational speed has a highly nonlinear characteristic. Although the rotational speed of the rotor can be varied by changing the frequencies of the input signals, it is difficult to control the rotational speed linearly.

2) Relationship Between Voltage and Rotational Speed: Fig. 9(b) shows the experimental relationship between the voltage and rotational speed. Only the voltage of the input signal for the second bending mode was varied, because the longitudinal vibration is mainly used as a clutch and does not provide much driving force. As can be seen from Fig. 9(b), rotational speed changes almost linearly as the input voltage changes. The rotor does not stop when the voltage is 0 V, because the contact points between the rotor and stator do not vibrate exactly along the z axis when only the first longitudinal mode is excited on the stator.

3) Relationship Between Phase Difference and Rotational Speed: Fig. 9(c) shows the experimental relationship between the phase difference and the rotational speed. The phase of the input signal for the first longitudinal mode was fixed at 0° and that for the second bending mode was varied. The positive and negative values of the rotational speed correspond to the rotational direction of the rotor. It can be seen from Fig. 9(c) that the relationship between the phase difference and the rotational speed has a highly nonlinear characteristic, however, the rotational speed can be varied by changing the phase difference of the input signals. In addition, it can be seen that the rotational direction of the rotor can be reversed continuously by changing the sign of the phase difference, because the rotational directions of the contact points on the stator are reversed, as shown in Fig. 5(c). The absolute value of the rotational speed increases as the absolute value of the phase difference increases, because the speed of the contact point becomes large, as also shown in Fig. 5(c).

4) Relationship Between Torque and Rotational Speed: Fig. 10 shows the experimental relationship between the torque and rotational speed when the normal load between the rotor and stator is varied. It can be seen from Fig. 10 that the rotational speed decreases as the torque increases, and that the maximum torque increases as the normal

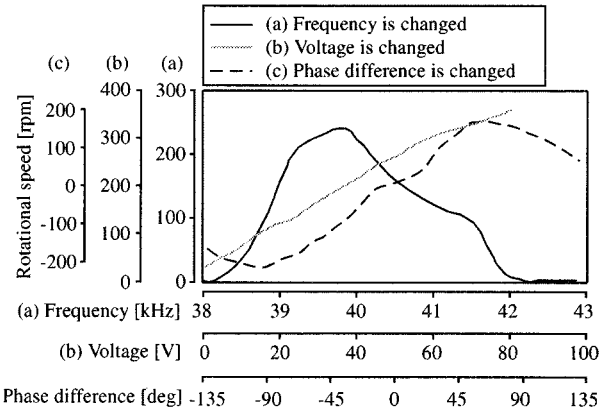

Fig. 9. Experimental results for open-loop control.

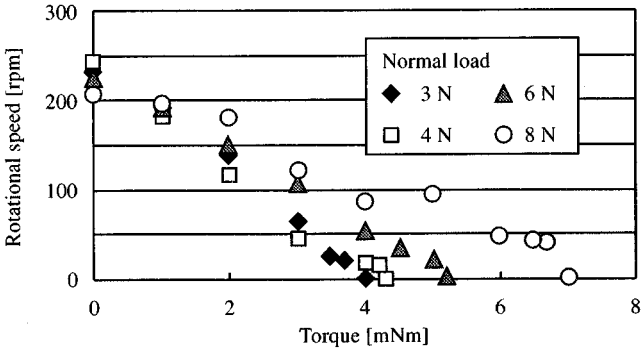

Fig. 10. Relationship between torque and rotational speed.

load between the rotor and stator increases. The maximum values of the rotational speed and the output torque under these conditions are about 250 r/min and 7 mNm, respectively. The estimated rotational speed and torque are about 400 r/min and 15 mNm as mentioned in Section II-B. The difference between the estimated and measured values was due to the following.

The estimated values were calculated under the assumption that there is no stiffness at the contact interface on the stator. However, at the contact interface, the rotor actually declines with respect to the stator. This causes the declinations as mentioned above [9], [10]. In addition, the coefficient of friction under the ultrasonic vibration becomes lower than that under normal condition [11].

B. Results for Closed-Loop Control Experiment

The experimental results for closed-loop control using the control method proposed in Section III-B are as follows. The basic experimental conditions are shown in Table I.

1) Speed Control: The step response of the rotational speed was measured using the device shown in Fig. 8(a). The desired rotational speed was 200 r/min, and the phase difference between the input signals was varied from -90 to 90° by (2). Fig. 11(a) shows the experimental results for the step response of the rotational speed when the proportional feedback gain K_p is 0.1. It can be seen from Fig. 11(a) that the rotational speed converged to the steady state, 200 r/min, after sufficient time, and there is no steady-state error. However, the rotational speed oscillates around 200 r/min because of initial rotor and stator deformation due to production tolerances. In the case of the

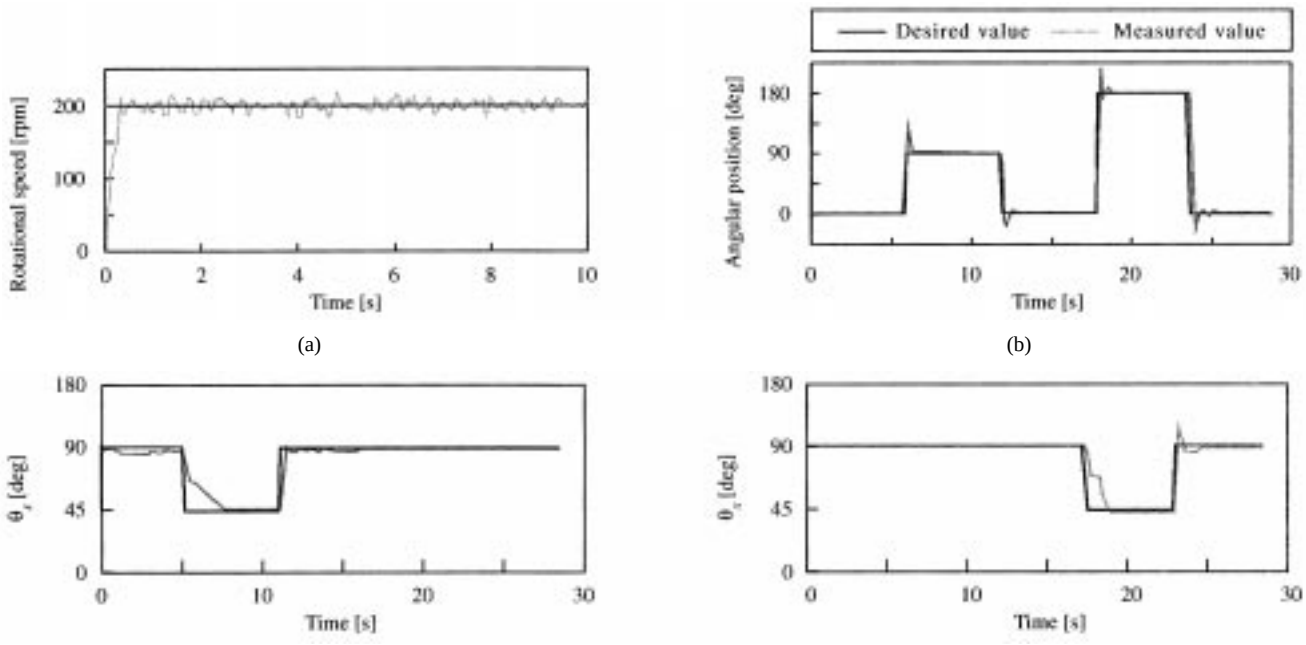

Fig. 11. Experimental results for closed-loop control. (a) Result for the speed control. (b) Result for the position control. (c) Results for multi-DOF position control.

standing wave ultrasonic motor, the oscillation of the rotational speed does not become perfectly periodical because the contact points on the rotor are not the same in each period. If the proportional feedback gain increases, it is seen that response time improves.

2) Position Control: The angular position was measured as it was incrementally varied in steps, using the measuring device shown in Fig. 8(a). The desired angular position varied with time from 0° to 90°, 0°, 180°, and 0°. The absolute value of the phase difference of the input signals was determined using the sigmoid function given in (3). Fig. 11(b) shows the experimental results of the step-wise response of angular position when the sigmoid function parameters α and M are 1.0 and 90, respectively. It can be seen from Fig. 11(b) that the angular position of the rotor was successfully moved to the desired position using the proposed control method. When the sigmoid function parameter α is greater than 1.0, overshoots occur.

3) Multi-DOF Position Control: The angular position of the rotor around the y axis was controlled successfully as described in Section V-B-2. Following this, the position control algorithm was extended to multi-DOF position control of the spherical rotor. The angular positions of the rotor around the x and y axis were measured using the multi-DOF position-sensing device shown in Fig. 8(b). The desired angular positions was varied with time from 90 to 45° and then back to 90°. Fig. 11(c) shows the experimental results for the multi-DOF position control when the sigmoid function parameters α and M are 1 and 30, respectively. It can be seen from Fig. 11(c) that the angular positions of the rotor around the x and y axes were successfully varied under control to the desired locations sequentially.

Now, it is confirmed that the angle of the rotor is controlled in perpendicular axes. Nonlinear and redundant characteristics of the multi-DOF ultrasonic motor should be clarified in the future study to understand the mixture of vibrations possibly provides unexpected driving forces against the rotor in order to drive the rotor around arbitrary axis.

VI. Discussion

A multi-DOF ultrasonic motor was proposed and constructed, and its motion was controlled successfully as described above. Therefore, the proposed driving principle of the multi-DOF ultrasonic motor was confirmed and the proposed control method worked successfully. The multi-DOF ultrasonic motor we developed has an important characteristic in addition to the characteristics of former ultrasonic motors. This characteristic, multi-DOF direct drive by a single motor, is so effective that it may replace the electromagnetic motor in the field of multi-DOF actuation. However, there are problems that remain to be solved in order to make the multi-DOF ultrasonic motor practical. These problems and their solutions are as follows.

Firstly, the output torque of the multi-DOF ultrasonic motor must be increased in order to use it in a robot arm joint. The ultrasonic motor is a frictionally driven motor, so it is necessary for increasing the output torque to optimize the contact condition between the rotor and stator: i.e., the relationship between the coefficient of friction, the stiffness, and the normal load must be optimized. The ultrasonic motor can essentially produce larger torque, so this problem can be solved by optimizing the parameters in (1).

Secondly, the multi-DOF angular position-sensing device must become smaller. The device shown in Fig. 8(b) needs a considerable amount of space, so a small sensing device, which is able to measure the multi-DOF motion of the spherical rotor, must be developed.

Fig. 12. The multi-DOF forceps.

Thirdly, the multi-DOF ultrasonic motor should be made smaller. The present diameter of the multi-DOF ultrasonic motor is 10 mm, however, it can be as small as a few millimeters by scaling it down analogously.

Fourthly, the performance of the closed-loop control system should be improved. For example, a controller for the driving frequency is needed in order to follow the natural frequencies of the vibrations even when the natural frequencies vary as a result of rising temperature or disturbance torque. The output voltage from the PZT plates for detecting the amplitude of the natural vibrations, shown in Fig. 4, must be monitored in order to observe the shift of the natural frequencies. Then the driving frequency can follow the natural frequencies of the vibration modes. For another example, the angular position around the perpendicular axis should be measured more precisely in order to control the rotor position more accurately.

If the problems mentioned above are solved, there are many applications of the multi-DOF ultrasonic motor in the field of robotics and mechatronics. For example, multi-DOF forceps for laparoscopic surgery can be constructed using a multi-DOF ultrasonic motor, in which the multi-DOF ultrasonic motor generates multi-DOF motion at the wrist.

Fig. 12 shows a prototype of multi-DOF forceps that we produced, where the open/shut motion at the tip is generated by a solenoid. The pre-load at the wrist is generated by the magnetic disk shown in Fig. 3. An important feature of the forceps is that no large operating gear is required outside the forceps. A simple multi-DOF forceps can be constructed using the multi-DOF ultrasonic motor. A multi-DOF endoscope and a robot eye are further examples of the possible applications. They can generate more dexterous motion than previous types, as well as being smaller and more silent.

VII. Conclusions

A multi-DOF ultrasonic motor that was developed by the authors is described in this paper. The conclusions of this study are as follows.

1) A driving principle for a multi-DOF ultrasonic motor, in which a multi-DOF ultrasonic motor uses the second bending vibrations and the first longitudinal vibration of a bar-shaped stator, was proposed;
2) A multi-DOF ultrasonic motor was designed using finite element analysis and then constructed;
3) A control method for the multi-DOF ultrasonic motor utilizing phase change is proposed. Then, the motion of the spherical rotor was successfully controlled using the proposed control method.

The authors will improve the characteristics of the multi-DOF ultrasonic motor in a future study in order to make it practical.

References

[1] T. Yano, "Multi-DOF actuators" (in Japanese), *J. Robot. Soc. Japan*, vol. 15, no. 3, pp. 330–333, 1997.
[2] R. Roth and K.-M. Lee, "Design optimization of a three degrees-of-freedom variable reluctance spherical wrist motor," *Trans. ASME J. Eng. Ind.*, vol. 117, pp. 378–388, 1995.
[3] T. Yano *et al.*, "Basic characteristics of the developed spherical stepping motor," in *Proc. IEEE/RSJ Int. Conf. Intelligent Robots and Systems*, vol. 3, 1999, pp. 1393–1398.
[4] R. Bansevicius, "Piezoelectric multi-degree of freedom actuators/sensors," in *Proc. 3rd Int. Conf. Motion and Vibration Control*, 1996, pp. K9–K15.
[5] T. Amano *et al.*, "An ultrasonic actuator with multi-degree of freedom using bending and longitudinal vibrations of a single stator," in *Proc. IEEE Int. Ultrasonics Symp.*, 1998, pp. 667–670.
[6] S. Toyama *et al.*, "Multi degree of freedom spherical ultrasonic motor," in *IEEE Int. Conf. Robotics and Automation*, 1995, pp. 2935–2940.
[7] K. Sasae *et al.*, "Development of a small actuator with three degrees of rotational freedom (2nd report)—Simulation and experiment of a friction drive" (in Japanese), *J. Japan Soc. Precis. Eng.*, vol. 61, no. 4, pp. 532–536, 1995.
[8] I. Okumura, "A design method of a bar-type ultrasonic motor for autofocus lenses," in *Proc. IFToMM-jc Int. Symp. Theory of Machines and Mechanisms*, 1992, pp. 75–80.
[9] T. Maeno *et al.*, "Finite element analysis of the rotor/stator contact in ring-type ultrasonic motor," *IEEE Trans. Ultrason. Ferroelect. Freq. Contr.*, vol. 39, pp. 668–674, Nov. 1992.
[10] T. Maeno, "Contact analysis of traveling wave type ultrasonic motor considering stick/slip condition" (in Japanese), *J. Acoust. Soc. Japan*, vol. 54, no. 4, pp. 305–311, 1998.
[11] H. Kanazawa *et al.*, "Tribology of ultrasonic motors" (in Japanese), *Tribologist*, vol. 38, no. 3, pp. 21–26, 1993.

Kenjiro Takemura received the B.S. degree in mechanical engineering and the M.S. degree in biomedical engineering from Keio University, Yokohama, Japan, in 1998 and 2000, respectively. He is currently working toward the Ph.D. degree in integrated design engineering at Keio University, Yokohama, Japan.

His current research focus is on ultrasonic motor and multi-DOF actuation.

Takashi Maeno received the B.S., M.S., and Ph.D. degrees in mechanical engineering from the Tokyo Institute of Technology, Tokyo, Japan, in 1984, 1986, and 1993, respectively.

From 1986 to 1995, he worked for Canon, Inc., Tokyo, Japan. From 1990 to 1992, he was a Visiting Industrial Fellow at the University of California, Berkeley. Since 1995, he has been with the Department of Mechanical Engineering at Keio University, Yokohama, Japan, where he is currently an Associate Professor.